Editors' Suggestion | Featured in Physics

Resonant Dipolar Collisions of Ultracold Molecules Induced by Microwave Dressing

Zoe Z. Yan,[1] Jee Woo Park,[2] Yiqi Ni,[1] Huanqian Loh,[3] Sebastian Will,[4] Tijs Karman,[5] and Martin Zwierlein[1]

[1]*MIT-Harvard Center for Ultracold Atoms, Research Laboratory of Electronics, and Department of Physics, Massachusetts Institute of Technology, Cambridge, Massachusetts 02139, USA*

[2]*Department of Physics, Pohang University of Science and Technology, Pohang 37673, Korea*

[3]*Department of Physics and Centre for Quantum Technologies, National University of Singapore, 117543 Singapore*

[4]*Department of Physics, Columbia University, New York 10027, USA*

[5]*ITAMP, Harvard-Smithsonian Center for Astrophysics, Cambridge, Massachusetts 02138, USA*

(Received 5 March 2020; revised 1 June 2020; accepted 22 June 2020; published 4 August 2020)

We demonstrate microwave dressing on ultracold, fermionic ^{23}Na^{40}K ground-state molecules and observe resonant dipolar collisions with cross sections exceeding 3 times the s-wave unitarity limit. The origin of these interactions is the resonant alignment of the approaching molecules' dipoles along the intermolecular axis, which leads to strong attraction. We explain our observations with a conceptually simple two-state picture based on the Condon approximation. Furthermore, we perform coupled-channel calculations that agree well with the experimentally observed collision rates. The resonant microwave-induced collisions found here enable controlled, strong interactions between molecules, of immediate use for experiments in optical lattices.

DOI: 10.1103/PhysRevLett.125.063401

Strong, long-range dipolar interactions turn ultracold molecules into a promising platform for simulating quantum many-body physics [1–5], precision measurements of fundamental constants [4,6,7], quantum computation [8–10], and quantum state-resolved chemistry [11–14]. Recent years have seen the production of several species of such dipolar molecular gases in the ultracold regime [14–22]. A common way to induce dipolar interactions in these systems is the application of static electric fields that align molecules in the laboratory frame. To acquire dipoles on the order of the molecule's body-frame moment d_0 requires fields on the order of $E \sim B_{\mathrm{rot}}/d_0 \sim \mathrm{kV/cm}$, where B_{rot} is the rotational constant. The presence and strength of the static electric field can be technically inconvenient.

In contrast, weak microwave electric fields that drive rotational transitions near resonance can lead to dipole moments on the order of the maximum value d_0. For example, dressing between the ground and first excited rotational states of a diatomic molecule yields dipole moments as large as the transition dipole moment for the electric dipole transition, $d_0/\sqrt{3}$, and thus dipolar interactions as large as $1/3$ of the maximum value at a given distance.

Induced interactions via microwave dressing of molecules is a crucial component of several proposals to create exotic states of matter in bulk [2,23–25] and lattice quantum gases [26,27]. In addition, standing-wave microwave fields in resonant cavities have been proposed to trap polar molecules [28–30]. Furthermore, engineering repulsive interactions via microwave dressing can potentially shield molecules from binary collisions [2,23,31–34], which limit the lifetime of bulk molecular gases in both chemically reactive [35,36] and nonreactive species [10,17,37–39] in the presence of trapping light [40–42]. Despite the promise of microwave dressing, its effect on collisional properties has not been studied thus far in ultracold dipolar molecules.

In this Letter, we observe strong microwave-induced interactions between fermionic ^{23}Na^{40}K molecules. The employed microwaves address the transition between the ground and the first excited rotational state. Microwave dressing enhances the probability for two molecules to reach short range, where they can undergo light-assisted chemical reactions in the presence of the trapping laser [40–42]; while ultimately this photoinduced loss can be eliminated by using repulsive box potentials [43,44], here the loss is employed as an efficient detector for the two-body collision cross section. We find that dressing leads to resonant dipolar collisions whereby the dipoles of approaching molecules align with the intermolecular axis. This results in strong attractive interactions even for microwave detunings larger than the Rabi coupling, which we explain using a two-state model based on the Condon approximation [45,46]. At all detunings, the collision cross sections are modeled quantitatively by coupled-channel calculations.

To start our experiment, we prepare a molecular gas in the absolute electronic, vibrational, rotational, and hyperfine ground state, as described in Refs. [19,37,47]. In short, ultracold atomic mixtures of ^{23}Na and ^{40}K are confined in an optical trap at 1064 nm and cooled to a temperature of $T = 560(80)$ nK. ^{23}Na^{40}K molecules are coherently

associated from this sample and initialized in the lowest vibrational, rotational, and hyperfine states of the ground electronic $X^1\Sigma^+$ manifold, with a peak density of $3.2(3) \times 10^{10}$ cm^{-3}. Without any external electromagnetic fields, ground state ^{23}Na^{40}K molecules have zero laboratory-frame dipole moment and experience no first-order dipole-dipole interaction. The dominant interaction is the background rotational van der Waals (vdW) interaction resulting from second-order dipolar coupling to the first rotationally excited state [19]. A microwave field near the resonance of the transition between the ground (rotational angular momentum quantum number $J = 0$) and the first excited ($J = 1$) rotational state is applied, thereby inducing a time-varying dipole moment in each molecule. The levels are spaced by the rotational splitting $2B_{\rm rot} = 5.643$ GHz, as shown in Fig. 1(a). Microwave dressing mixes opposite parity rotational states and imparts a significant fraction of the full dipole moment $d_0 = 2.7$ D to the molecules. Tuned to the transition between $J = 0$ and $J = 1$, a resonant circularly polarized microwave field induces a dipole moment of $d_0/\sqrt{6} \approx 1.1$ D [24,48], rotating with the microwave electric field. The different hyperfine states of the first rotationally excited manifold are identified through microwave spectroscopy [37]. States are described in the nuclear-spin uncoupled basis $|J, m_J, m_{I_{\rm Na}}, m_{I_{\rm K}}\rangle$, which is an eigenbasis for the $J = 0$, $m_J = 0$ manifold.

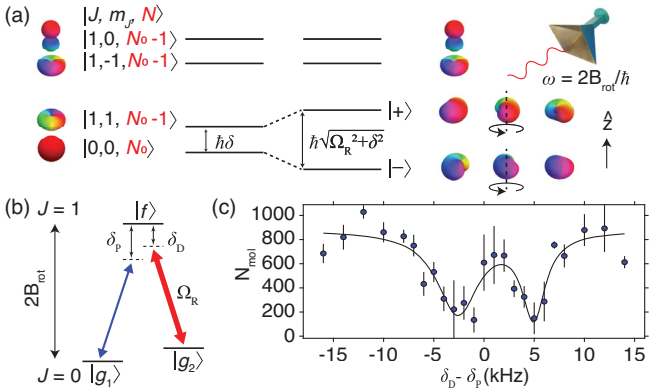

FIG. 1. Microwave dressing in ^{23}Na^{40}K. (a) Schematic energy level diagram, labeled by rotational quantum numbers J, m_J and microwave photon number N. Hyperfine structure is omitted for simplicity. The rotational ground state $|J = 0, m_J = 0\rangle$ is coupled by a σ^+-polarized microwave field to the lowest energy state in the $J = 1$ manifold, $|1, 1\rangle$, resulting in dressed states $|-\rangle, |+\rangle$. Higher-lying "spectator" states (i.e., $|1, 0\rangle$ and $|1, -1\rangle$) are not coupled by the microwaves. Molecular wave functions are depicted with color encoding the wave function's phase. (b) Level scheme with the relevant molecular states for Autler-Townes spectroscopy. A microwave field with Rabi frequency $\Omega_R/2\pi = 7$ kHz is used to address the $|g_2\rangle \to |f\rangle$ transition. The weaker probe microwave field has a frequency detuning δ_P that is scanned around the $|g_1\rangle \to |f\rangle$ transition. (c) An Autler-Townes doublet is observed when we scan the probe microwave. The solid line shows a double Lorentzian fitted to the line shape.

States in $J = 1$ are hyperfine-mixed superpositions of these basis states [37]. Therefore, a microwave field with well-defined polarization can couple the absolute ground hyperfine state, $|g_1\rangle \equiv |0, 0, -4, 3/2\rangle$, to multiple $J = 1$ states. Furthermore, the microwave antenna produces radiation at all polarizations: π, σ^+, and σ^- [48]. The 1064 nm trap polarization has been tuned to a "magic" condition that limits differential ac Stark shifts to < 1 kHz [48].

To demonstrate the presence of microwave dressing, we induce an Autler-Townes splitting of the $J = 0 \to J = 1$ transition. A microwave field with Rabi frequency $\Omega_R/2\pi = 7$ kHz is applied on resonance with the transition between $|g_2\rangle \equiv |0, 0, -3, 3/2\rangle$ and $|f\rangle$, predominantly equal to $|1, 0, -4, 3/2\rangle$, as shown in Fig. 1(b). This dressing field induces a splitting of the excited state, which is probed by scanning the frequency of a weaker microwave tuned near the $|g_1\rangle \to |f\rangle$ transition. We observe an Autler-Townes doublet as shown in Fig. 1(c), demonstrating that the $|g_1\rangle$ state is depleted by the probe field only when it is tuned to the dressed resonances.

We find that microwave dressing dramatically enhances molecular interactions. Although ^{23}Na^{40}K should not experience two-body collisional loss in its electronic and vibrational ground state, the trapping laser at 1064 nm leads to photoinduced loss at short range [40]. We employ this loss mechanism as a probe for microwave-induced two-body collisions. To start, the dressing microwave field is first applied with a frequency far below the lowest rotational resonance, the $|g_1\rangle \to |f\rangle$ transition. Here, and for the remainder of the Letter, $|f\rangle$ represents the lowest energy $J = 1$ state, which has predominantly $|1, 1, -4, 3/2\rangle$ character. The frequency is then swept adiabatically from the initial detuning $\delta_{\rm initial}$, where the molecule in the lower dressed eigenstate $|-\rangle$ has predominantly $|g_1\rangle$ character, to a detuning $\delta_{\rm final}$ near or on the dressed resonance [see Fig. 2(a)]. Figure 1(a) depicts the dressed eigenstate $|-\rangle$, which is a superposition of the states $|g_1\rangle$ and $|f\rangle$. The red-detuned microwaves avoid driving other hyperfine transitions during the sweep [the spectator states of Fig. 1(a)]; the next higher $J = 1$ state lies 27 kHz above the $|f\rangle$ state. The microwave field is held at its final detuning for a varying amount of time, allowing collisions to occur, before the detuning is swept back to $\delta_{\rm initial}$ and the remaining $|g_1\rangle$ molecules are imaged.

We observe the evolution of the molecule number in $|g_1\rangle$ as a function of hold time to extract the loss rate of the ensemble; examples for certain detunings are shown in Fig. 2(b). The loss curves are fit to a two-body decay model, where the density $n(t)$ as a function of time obeys $n(t) = n_0/(1 + \beta n_0 t)$. Here, n_0 is the initial average molecule density and β is the two-body loss coefficient. The microwave dressing shortens the sample lifetime by orders of magnitude, compared to the $\sim$3 s lifetime in the absence of microwaves [19,37,48]. Since both molecules involved in the collision will be lost, the loss rate is related

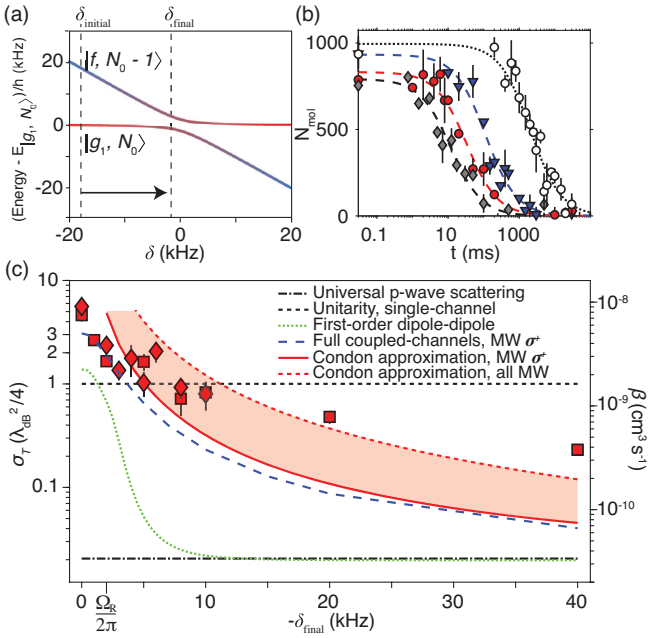

FIG. 2. Observation of resonant dipolar collisions between dressed molecules. (a) Dressed energies as a function of the microwave frequency detuning δ from the $|g_1\rangle \rightarrow |f\rangle$ transition at 129 G. δ is swept from far off-resonance (typically 12 kHz below δ_{final}) to a final detuning at a rate of 3 kHz ms^{-1} and held for a varying hold time t. (b) Evolution of the molecule number under microwave dressing with $\Omega_R/2\pi = 1.7$ kHz for $\delta_{\mathrm{final}} = -20, -5$, and 0 kHz (in blue triangles, red circles, and gray diamonds). A lifetime curve of $|g_1\rangle$ taken without microwaves is shown with open circles. Dashed lines are two-body decay fits. (c) Collision rates (left axis) obtained from loss coefficients (right axis) of dressed molecules as a function of δ_{final} for $\Omega_R/2\pi = 1.7$ kHz (squares) and 2.4 kHz (diamonds). The black dot-dashed line shows the universal p-wave loss at 560 nK [54], and the green dotted line includes the additional loss from first-order dipole-dipole interactions. The unitarity limit for the loss rate from a single partial wave is shown as the black dashed line. The blue dashed line shows the coupled-channel prediction, assuming pure σ^+ microwave polarization, and the red line depicts the rate given by the Condon approximation. Including all microwave (MW) polarizations, the Condon approximation increases to the red dashed line.

to the two-body scattering cross section σ by $\beta = 2\langle\sigma v\rangle$, where $\langle\cdots\rangle$ denotes the ensemble average and v the relative velocity of colliding molecules. We therefore define a thermally averaged scattering cross section $\sigma_{\mathrm{T}} = \beta/2\langle v\rangle$, with $\langle v\rangle = \sqrt{8k_BT/\pi\mu}$ the average relative velocity and $\mu = (m_{\mathrm{Na}} + m_{\mathrm{K}})/2$ the reduced mass.

Figure 2(c) shows the measured collision cross section (red data points, left axis) and associated loss rate (right axis) as a function of microwave detuning. The resonant scattering rate is an order of magnitude larger than rates found in previous experiments [38,39,55]. Away from resonance, the scattering cross section is reduced but remains orders of magnitude larger than that of both of the bare $|g_1\rangle$ and $|f\rangle$ states in the absence of microwaves. The bare states feature loss rates of only $\beta^{(\mathrm{bare})} = 2 \times 10^{-11}$ cm^3 s^{-1} [19,37] close to the universal loss rate of $\beta^{(\mathrm{universal})} = 3 \times 10^{-11}$ cm^3 s^{-1} [54], which reflects the loss when the molecules experience vdW interactions only under p-wave collisions.

To emphasize how strongly microwave dressing can modify interactions, the comparison to the s-wave unitarity limit is useful. A single partial wave contributes at most the unitarity limit, $\sigma^{(\mathrm{unitarity})} = \lambda_{\mathrm{dB}}^2/4$, limited by the de Broglie wavelength $\lambda_{\mathrm{dB}} = \sqrt{2\pi\hbar^2/\mu k_B T}$, corresponding to a loss rate $\beta^{(\mathrm{unitarity})} = 2\hbar\lambda_{\mathrm{dB}}/\mu = 1.7 \times 10^{-9}$ cm^3 s^{-1}. For ultracold bosons that undergo only s-wave collisions, $\sigma^{(\mathrm{unitarity})}$ and $\beta^{(\mathrm{unitarity})}$ are upper limits to the collisional cross section and loss rate, respectively. For ultracold fermions such as ^{23}Na^{40}K, one might expect the p-wave centrifugal barrier to prevent molecules from reaching short range and thus reduce losses, but the dipole-dipole interaction suppresses this barrier. For dressing on a σ^+ resonance, the first-order dipole-dipole interaction is attractive for $M_L = \pm 1$, where M_L is the projection of the molecules' relative angular momentum [48], leading to a p-wave loss rate that is at most twice the unitarity limit.

In the remainder of the Letter, we explain the origins of the dressing-induced collisions. We first consider a simple description where the molecules in the $|-\rangle$ state experience only background vdW interactions and the first-order dipole-dipole interaction, neglecting all "spectator states" and the upper dressed state $|+\rangle$. In this approximation, the molecular dipole moments always align with the rotating electric field. We calculate the scattering wave function subject to an absorbing boundary condition at short range that models photoinduced loss [48]. The resulting loss curve, shown as the green dotted line in Fig. 2(c), is comparable to the unitarity limit near resonance. Away from resonance where $|\delta_{\mathrm{final}}| \gg \Omega_R/2\pi$, microwave dressing induces a negligible dipole moment, and in this first-order approximation the collision rate rapidly decreases to the universal limit. This disagrees with the experimental loss rates, which remain an order of magnitude higher than the bare rate without microwave dressing even for detunings greater than Ω_R. Thus, the first-order dipole-dipole effect is insufficient to explain the enhanced collision rates.

Next, we consider contributions from the upper dressed state $|+\rangle$, restricting the two-molecule basis to $|--\rangle$ and $(|+-\rangle + |-+\rangle)/\sqrt{2}$, written as $|-+\rangle$ for convenience in the remainder of the Letter. This approximation is valid at detunings greater than Ω_R when accounting only for σ^+ microwave polarization and neglecting the presence of spectator states $|J = 1, m_J = 0\rangle$ and $|1, -1\rangle$. Neglecting these spectators, the dipoles can only ever point in the direction of the rotating microwave electric field, i.e., in the x-y plane, as they approach each other at close range. The interactions will thus be repulsive if molecules meet along the z direction ($M_L = 0$) and attractive if they meet in the

x-y plane, i.e., for $M_L = \pm 1$. One might therefore expect a maximum p-wave cross section of at most *twice* the unitarity limit corresponding to the two attractive $M_L = \pm 1$ channels for thermal energies far greater than the barrier height. For red detunings exceeding the Rabi frequency, the adiabatic potential curves for $L = 1$, $M_L = 1$ display an avoided crossing between the incoming centrifugal potential $\sim \hbar^2/\mu R^2$, with negligible dipolar interaction, and the attractive potential $\sim -h\delta_{\text{final}} - d_0^2/12R^3 + \hbar^2/\mu R^2$ [see Fig. 3(a)], corresponding to the time-averaged dipolar attraction of two classical rotating dipoles of strength $d_0/\sqrt{6}$ approaching in the plane of rotation. The diabatic potentials cross at the Condon point R_C, and the effective Rabi coupling between the states is visualized by the avoided crossing of the adiabatic curves.

However, a quantitative comparison to the data requires treating the spectators $|J = 1, m_J = 0\rangle$ and $|1, -1\rangle$, as they are sufficiently close in energy. These spectators enable the molecules to reorient so that their dipoles point head to tail [see Fig. 3(b)], leading to resonant dipole-dipole interactions. This occurs when the dipolar energy overcomes the energy difference between the dressed incoming state and the state of attractively interacting molecules or, classically, when the electric field applied by one molecule on the other exceeds the electric field of the applied microwaves. Thus, at short range the interaction between two microwave-dressed molecules incoming in the lowest internal state $|--\rangle$ will always be attractive regardless of which direction the molecules meet along, i.e., for all three M_L components, giving a potential $\sim -2d_0^2/3R^3$. This resonant dipolar collision leads to p-wave loss as high as *3 times* the unitarity limit. Even faster losses require inclusion of higher partial waves, $L > 1$. Compared to the spectator-free case of Fig. 3(a), the Condon point is moved outward. Losses can be analytically derived for detunings exceeding the Rabi frequency by the reflection approximation for the Franck-Condon overlap [45,46,56],

$$\beta = \frac{16\pi^2}{9\hbar}\frac{\Omega_R^2}{\delta^2} d_0^2 \langle j_l(kR_C)^2 \rangle, \tag{1}$$

where the angular brackets indicate averaging over the thermal velocity distribution, k is the collision wave vector, and j_l is the spherical Bessel function of the first kind. The resulting approximation is shown as the solid red line in Fig. 2(c).

For a full model of the observed loss curves we employ coupled-channel (CC) calculations [48] [see the dashed blue line in Fig. 2(c)]. The molecules are represented as rigid rotors with hyperfine structure that interact through dipole-dipole interactions, undergo photoinduced loss at short range, and can scatter inelastically into field-dressed levels other than the initial $|-\rangle$ state. The scattering calculations capture both the high loss rate on resonance, exceeding 3 times the s-wave unitarity limit, and the slow

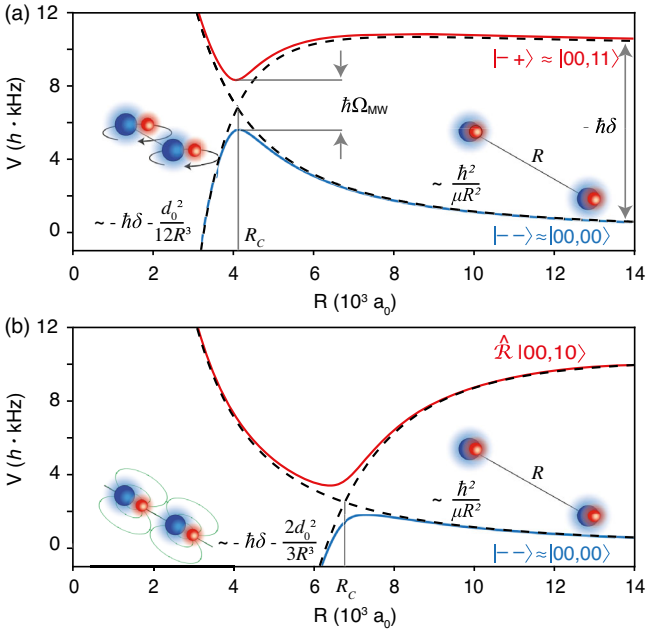

FIG. 3. Two-state picture of dipolar interactions between microwave-dressed molecules, valid for detunings larger than the Rabi coupling and shown here for $M_L = 1$. (a) Interaction potentials for molecules in the $|--\rangle$ and $|-+\rangle$ states. An effective microwave Rabi coupling between the branches causes an avoided crossing at R_C. Excluding spectator states, the molecules remain aligned with the microwave field. Ω_{MW} is the effective Rabi frequency between the two states, proportional to Ω_R [48]. (b) The same as (a) but including spectator states: the relevant excited potential comes from two molecules in the $\hat{\mathcal{R}}(|00\rangle|10\rangle + |10\rangle|00\rangle)/\sqrt{2}$ state [48], which represents the molecules aligning at short range along the intermolecular axis $\hat{R}$. Here, molecules experience strong, resonant dipole-dipole interactions.

decrease with detuning: even at $|\delta_{\text{final}}| \gg \Omega_R/2\pi \approx 2$ kHz, the loss is significantly higher than the universal loss rate, obtained without microwave dressing. However, the experimentally observed loss decreases even more slowly with detuning than for CC calculations that include only σ^+ polarization. We attribute this to the π and σ^- components of the microwave field [48]. On the σ^+ resonance, these field components address far-detuned hyperfine transitions, and their effect can be neglected. Away from resonance, however, these field components should contribute comparably and hence double the effective Rabi frequency [48]. This effect is also incorporated into the Condon approximation, resulting in the red dashed line in Fig. 2(c). The adjusted Condon approximation matches the experiment at higher detunings.

The dressing-induced collisions are affected by hyperfine interactions that shift the spectator states relative to the state used for microwave dressing. Recall that the maximum strength of resonant dipolar interactions is given by the full transition dipole matrix element of the dressed transition. This requires reorientation of the molecules

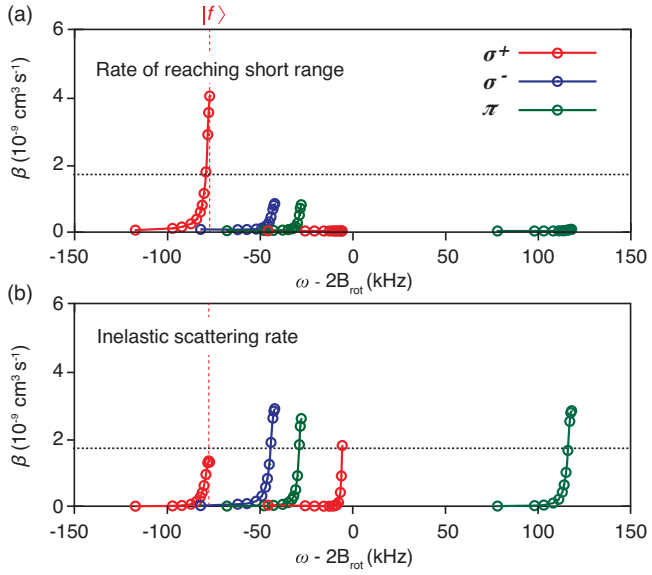

FIG. 4. Hyperfine-state-dependent interactions, calculated at 129 G. (a) The short-range loss, which occurs when the incoming molecules reach the absorptive boundary condition that models photoinduced loss, is strongest for the lowest hyperfine state $|f\rangle$, whereas (b) excited hyperfine states have larger inelastic loss due to transitions to different field-dressed levels and hyperfine states. The single-channel unitarity limit is shown as the dotted line.

along their intermolecular axis and thus inclusion of the relevant $|J, m_J\rangle$ states, typically split by the hyperfine interaction. Hence, resonant interactions take full effect when the dipole-dipole interaction is large compared to the hyperfine splittings.

Though here the microwave dressing was on the lowest $J = 1$ state, the choice to dress on a higher hyperfine state would affect the induced collision rates. Potential curves for dressing on states higher than $|f\rangle$ exhibit many crossings rather than approaching an isolated attractive resonant dipole-dipole potential [48], leading to slower scattering rates to reach short range [Fig. 4(a)]. Additionally, nonadiabatic transitions into lower-lying hyperfine states may increase the inelastic losses of the reflected flux to hyperfine states other than the initial channel, compared to the case of dressing on $|f\rangle$ [Fig. 4(b)].

State-dependent resonant dipolar interactions induced by microwave dressing found here will enrich applications of polar molecules in quantum computation and simulation of many-body physics [1–4]. The characteristic range R_C where the resonant dipolar collision occurs is directly controlled by the microwave detuning. This range can easily reach the typical spacings in optical lattices, ~500 nm, enabling dipolar exchange energies to dominate over all other relevant energy scales in the system. Here we observed dressing through collisional losses, but under appropriate conditions (e.g., molecules trapped in a repulsive optical "box" potential) the short-range photoinduced losses should not occur. In such situations, microwave and electric field dressing can lead to strong elastic scattering, offering a powerful technique to tune intermolecular interactions. Understanding and harnessing such interactions in ultracold polar molecules will be crucial for the creation of novel phases of matter, including topological superfluidity [24].

We would like to thank Alexey Gorshkov for the stimulating discussions. This work was supported by the NSF, AFOSR, ARO, an AFOSR Multidisciplinary University Research Initiatives (MURI) on "Exotic Phases of Matter," the David and Lucile Packard Foundation, the Vannevar Bush Faculty Fellowship, and the Gordon and Betty Moore Foundation through Grant No. GBMF5279. Z. Z. Y. acknowledges support from the NSF GRFP. T. K. acknowledges support from NWO Rubicon Grant No. 019.172EN.007 and a NSF grant to ITAMP. S. W. acknowledges support from the Alfred P. Sloan Foundation. H. L. acknowledges support from the National Research Foundation Singapore.

[1] A. Micheli, G. K. Brennen, and P. Zoller, Nat. Phys. **2**, 341 (2006).
[2] H. P. Büchler, E. Demler, M. Lukin, A. Micheli, N. Prokof'ev, G. Pupillo, and P. Zoller, Phys. Rev. Lett. **98**, 060404 (2007).
[3] G. Pupillo, A. Griessner, A. Micheli, M. Ortner, D. W. Wang, and P. Zoller, Phys. Rev. Lett. **100**, 050402 (2008).
[4] R. V. Krems, W. C. Stwalley, and B. Friedrich, *Cold Molecules: Theory, Experiment, Applications* (CRC Press, Boca Raton, 2009).
[5] B. Yan, S. A. Moses, B. Gadway, J. P. Covey, K. R. Hazzard, A. M. Rey, D. S. Jin, and J. Ye, Nature (London) **501**, 521 (2013).
[6] L. D. Carr, D. DeMille, R. V. Krems, and J. Ye, New J. Phys. **11**, 055049 (2009).
[7] V. Andreev *et al.* (ACME Collaboration), Nature (London) **562**, 355 (2018).
[8] D. DeMille, Phys. Rev. Lett. **88**, 067901 (2002).
[9] S. F. Yelin, K. Kirby, and R. Côté, Phys. Rev. A **74**, 050301 (R) (2006).
[10] J. W. Park, Z. Z. Yan, H. Loh, S. A. Will, and M. W. Zwierlein, Science **357**, 372 (2017).
[11] R. V. Krems, Phys. Chem. Chem. Phys. **10**, 4079 (2008).
[12] G. Quéméner and P. S. Julienne, Chem. Rev. **112**, 4949 (2012).
[13] N. Balakrishnan, J. Chem. Phys. **145**, 150901 (2016).
[14] H. Yang, D.-C. Zhang, L. Liu, Y.-X. Liu, J. Nan, B. Zhao, and J.-W. Pan, Science **363**, 261 (2019).
[15] K. K. Ni, S. Ospelkaus, M. H. De Miranda, A. Pe'er, B. Neyenhuis, J. J. Zirbel, S. Kotochigova, P. S. Julienne, D. S. Jin, and J. Ye, Science **322**, 231 (2008).
[16] J. G. Danzl, M. J. Mark, E. Haller, M. Gustavsson, R. Hart, J. Aldegunde, J. M. Hutson, and H. C. Nägerl, Nat. Phys. **6**, 265 (2010).

[17] T. Takekoshi, L. Reichsöllner, A. Schindewolf, J. M. Hutson, C. R. Le Sueur, O. Dulieu, F. Ferlaino, R. Grimm, and H. C. Nägerl, Phys. Rev. Lett. **113**, 205301 (2014).
[18] P. K. Molony, P. D. Gregory, Z. Ji, B. Lu, M. P. Köppinger, C. R. Le Sueur, C. L. Blackley, J. M. Hutson, and S. L. Cornish, Phys. Rev. Lett. **113**, 255301 (2014).
[19] J. W. Park, S. A. Will, and M. W. Zwierlein, Phys. Rev. Lett. **114**, 205302 (2015).
[20] M. Guo, B. Zhu, B. Lu, X. Ye, F. Wang, R. Vexiau, N. Bouloufa-Maafa, G. Quéméner, O. Dulieu, and D. Wang, Phys. Rev. Lett. **116**, 205303 (2016).
[21] T. M. Rvachov, H. Son, A. T. Sommer, S. Ebadi, J. J. Park, M. W. Zwierlein, W. Ketterle, and A. O. Jamison, Phys. Rev. Lett. **119**, 143001 (2017).
[22] F. Seeßelberg, N. Buchheim, Z.-K. Lu, T. Schneider, X.-Y. Luo, E. Tiemann, I. Bloch, and C. Gohle, Phys. Rev. A **97**, 013405 (2018).
[23] A. Micheli, G. Pupillo, H. P. Büchler, and P. Zoller, Phys. Rev. A **76**, 043604 (2007).
[24] N. R. Cooper and G. V. Shlyapnikov, Phys. Rev. Lett. **103**, 155302 (2009).
[25] J. Levinsen, N. R. Cooper, and G. V. Shlyapnikov, Phys. Rev. A **84**, 013603 (2011).
[26] M. L. Wall and L. D. Carr, Phys. Rev. A **82**, 013611 (2010).
[27] A. V. Gorshkov, S. R. Manmana, G. Chen, J. Ye, E. Demler, M. D. Lukin, and A. M. Rey, Phys. Rev. Lett. **107**, 115301 (2011).
[28] D. DeMille, D. R. Glenn, and J. Petricka, Eur. Phys. J. D **31**, 375 (2004).
[29] D. P. Dunseith, S. Truppe, R. J. Hendricks, B. E. Sauer, E. A. Hinds, and M. R. Tarbutt, J. Phys. B **48**, 045001 (2015).
[30] S. C. Wright, T. E. Wall, and M. R. Tarbutt, Phys. Rev. Research **1**, 033035 (2019).
[31] M. L. González-Martínez, J. L. Bohn, and G. Quéméner, Phys. Rev. A **96**, 032718 (2017).
[32] A. V. Gorshkov, P. Rabl, G. Pupillo, A. Micheli, P. Zoller, M. D. Lukin, and H. P. Büchler, Phys. Rev. Lett. **101**, 073201 (2008).
[33] T. Karman and J. M. Hutson, Phys. Rev. Lett. **121**, 163401 (2018).
[34] L. Lassablière and G. Quéméner, Phys. Rev. Lett. **121**, 163402 (2018).
[35] S. Ospelkaus, K.-K. Ni, D. Wang, M. H. G. de Miranda, B. Neyenhuis, G. Quéméner, P. S. Julienne, J. L. Bohn, D. S. Jin, and J. Ye, Science **327**, 853 (2010).
[36] X. Ye, M. Guo, M. L. González-Martínez, G. Quéméner, and D. Wang, Sci. Adv. **4**, eaaq0083 (2018).
[37] S. A. Will, J. W. Park, Z. Z. Yan, H. Loh, and M. W. Zwierlein, Phys. Rev. Lett. **116**, 225306 (2016).
[38] M. Guo, X. Ye, J. He, M. L. González-Martínez, R. Vexiau, G. Quéméner, and D. Wang, Phys. Rev. X **8**, 041044 (2018).
[39] P. D. Gregory, M. D. Frye, J. A. Blackmore, E. M. Bridge, R. Sawant, J. M. Hutson, and S. L. Cornish, Nat. Commun. **10**, 3104 (2019).
[40] A. Christianen, M. W. Zwierlein, G. C. Groenenboom, and T. Karman, Phys. Rev. Lett. **123**, 123402 (2019).
[41] P. D. Gregory, J. A. Blackmore, S. L. Bromley, and S. L. Cornish, Phys. Rev. Lett. **124**, 163402 (2020).
[42] Y. Liu, M.-G. Hu, M. Nichols, D. Grimes, T. Karman, H. Guo, and K.-K. Ni, arXiv:2002.05140.
[43] A. L. Gaunt, T. F. Schmidutz, I. Gotlibovych, R. P. Smith, and Z. Hadzibabic, Phys. Rev. Lett. **110**, 200406 (2013).
[44] B. Mukherjee, Z. Yan, P. B. Patel, Z. Hadzibabic, T. Yefsah, J. Struck, and M. W. Zwierlein, Phys. Rev. Lett. **118**, 123401 (2017).
[45] P. S. Julienne, J. Res. Natl. Inst. Stand. Technol. **101**, 487 (1996).
[46] C. Boisseau, E. Audouard, J. Vigué, and P. S. Julienne, Phys. Rev. A **62**, 052705 (2000).
[47] J. W. Park, S. A. Will, and M. W. Zwierlein, New J. Phys. **17**, 075016 (2015).
[48] See Supplemental Material at http://link.aps.org/supplemental/10.1103/PhysRevLett.125.063401, which contains Refs. [49–53], for further details on the experimental procedure, coupled channel calculations, interaction potentials, and the Condon approximation.
[49] L. M. C. Janssen, A. van der Avoird, and G. C. Groenenboom, Phys. Rev. Lett. **110**, 063201 (2013).
[50] J. Aldegunde and J. M. Hutson, Phys. Rev. A **96**, 042506 (2017).
[51] J. Aldegunde, B. A. Rivington, P. S. Żuchowski, and J. M. Hutson, Phys. Rev. A **78**, 033434 (2008).
[52] S. Kotochigova (private communication).
[53] A. Christianen, T. Karman, R. A. Vargas-Hernandez, G. C. Groenenboom, and R. V. Krems, J. Chem. Phys. **150**, 064106 (2019).
[54] Z. Idziaszek and P. S. Julienne, Phys. Rev. Lett. **104**, 113202 (2010).
[55] K. K. Ni, S. Ospelkaus, D. Wang, G. Quéméner, B. Neyenhuis, M. H. De Miranda, J. L. Bohn, J. Ye, and D. S. Jin, Nature (London) **464**, 1324 (2010).
[56] K. Burnett, P. S. Julienne, and K.-A. Suominen, Phys. Rev. Lett. **77**, 1416 (1996).